MOLECULAR AND CELLULAR BIOLOGY, Nov. 1992, p. 5174–5188
0270-7306/92/115174-15$02.00/0

Vol. 12, No. 11

Temporal Order of DNA Replication in the *H-2* Major Histocompatibility Complex of the Mouse

EDWARD G. SPACK,* E. DIANN LEWIS, BRIAN PARADOWSKI, ROBERT T. SCHIMKE, AND PATRICIA P. JONES

Department of Biological Sciences, Stanford University, Stanford, California 94305

Received 9 March 1992/Returned for modification 4 June 1992/Accepted 13 August 1992

As an approach to mapping replicons in an extended chromosomal region, the temporal order of DNA replication was analyzed in the murine major histocompatibility gene complex (MHC). Replicating DNA from T-lymphoma and myelomonocyte cell lines was density labeled with bromodeoxyuridine and extracted from cells which had been fractionated into different stages of S phase by centrifugal elutriation. The replicating DNA from each fraction of S phase was separated from nonreplicating DNA on density gradients, blotted, and hybridized with 34 specific MHC probes. The earliest replication occurred in the vicinity of transcribed genes *K*, *HAM1* and *HAM2*, *RD*, *B144*, *D*, *L*, *T18*, and *T3*. The temporal order of replication of groups of DNA segments suggests the location of five or six replicons within the *H-2* complex, some of which appear to be either unidirectional or markedly asymmetric. The rates of replication through each of these apparent replicons appear to be similar. The *TL* region of the S49.1 T-lymphoma cells, which contains at least three transcribed genes, replicates earlier than the inactive *TL* region of WEHI-3 myelomonocytic cells. These results provide further evidence of a relationship between transcription and the initiation of DNA replication in mammalian cells. The mouse MHC examined in this study is the largest chromosomal region (>2,000 kb) measured for timing of replication to date.

Initiation of DNA replication occurs at specific sequences in viruses, bacteria, and yeasts, but genomic complexity has hindered efforts to map precisely the organization of DNA replication in higher eukaryotes. The gross organization of mammalian replication was first revealed by differential labeling and fiber autoradiography (reviewed in references 19, 27, 33, and 70). These studies demonstrated that different chromosomal regions replicate at distinct times during S phase (25, 26) and that this regulated timing of replication is maintained over successive cell cycles. The units of replication (termed replicons) are generally 50 to 330 kb, and clusters of up to 100 replicons may initiate replication simultaneously. The number of replicons may vary with developmental stage in some eukaryotes. For example, certain insects and amphibian embryonic cells complete S phase more rapidly than do adult cells by initiating replication from a greater number of active origins (4). The period of S phase in which a particular gene is replicated may also be altered by translocation or transcription (10, 18, 25, 30). Thus, the number of active origins of replication and the timing of their initiation can vary in eukaryotic cells.

In the two decades since the general parameters of mammalian DNA replication were established by fiber autoradiography, numerous gene regions have been mapped, but the organization of mammalian replicons has been examined in few specific extended gene complexes. The size of the mammalian genome and the instability of autonomous mammalian sequences have hindered efforts to identify replicons in single-copy gene regions. Some of the problems inherent in analyzing single-copy sequences have been overcome by examining amplified genes, such as the 1,000-fold-amplified dihydrofolate reductase (DHFR) domain of methotrexate-resistant Chinese hamster ovary cells. Several studies have identified two putative origins of replication within a 28-kb region downstream of the DHFR gene (2, 12, 28, 44), with one possible initiation site localized within a 0.45-kb sequence (8, 9). However, analysis of replication intermediates by two-dimensional gel electrophoresis suggests that replication can start at random sites within the 28-kb initiation zone (43, 72).

Techniques used to identify the precise location of replication origins are best applied to relatively short regions of DNA (several hundred kilobases). Therefore, characterization of the organization of replicons and their origins in extended chromosomal regions requires initial identification of the approximate locations of origins by using a low-resolution approach. Several years ago, Schildkraut and colleagues developed a technique to determine the relative order of replication in a single-copy gene region and by inference to locate approximate origins of replication (10, 24). Their approach combined density labeling of replicating DNA, fractionation of S-phase cells by centrifugal elutriation, and comparison of relative levels of hybridization of specific probes to each S-phase subfraction. This method demonstrated the temporal order of replication and predicted the replicon organization of the mouse immunoglobulin heavy-chain (IgH) and globin gene complexes (7, 18, 24). Other recent studies have begun to characterize replication in the human *c-myc* (41) and cystic fibrosis (59) gene loci. However, knowledge of the organization of replicons in extended chromosomal regions remains limited.

In this study, we have determined the relative timing of replication of DNA segments in the *H-2* major histocompatibility complex (MHC) of the mouse, using the methods of Schildkraut and colleagues as a first step in characterizing replicons in this extended gene region. This multigene family encodes several classes of proteins with crucial roles in the immune system (Table 1) and offers several advantages for the characterization of mammalian replication. The *H-2*

* Corresponding author.

TABLE 1. *H-2* gene expression and function

Region	Gene[a]	Protein name	Encoded protein[b]	Tissue expression	Function
K	*K*	K (class I)	45 kDa; TM; hd w/β2M	Virtually all nucleated cells	Binds endogenous peptides for recognition by the variable T-cell receptor of $CD8^+$ T lymphocytes (cytotoxic and suppressor cells)
	K2	None (pseudogene)			
I	*Pb*	None (pseudogene)			
	HAM1	Histocompatibility antigen modifier 1	63 kDa; TM	Virtually all nucleated cells	Putative peptide transporter
	HAM2	Histocompatibility antigen modifier 2	63 kDa; TM	Virtually all nucleated cells	Putative peptide transporter
	Ab	Aβ (class II)	29 kDa; TM; hd w/Aα	B lymphocytes, activated T lymphocytes, macrophages, dendritic cells	Aa:Ab and Ea:Eb heterodimers bind exogenous peptides for recognition by the variable T-cell receptor of $CD4^+$ T lymphocytes (helper cells)
	Aa	Aα (class II)	34 kDa; TM; hd w/Aβ	Same as *Aβ*	Same as *Aβ*
	Eb	Eβ (class II)	29 kDa; TM; hd w/Eα	Same as *Aβ*	Same as *Aβ*
	Ea	Eα (class II)	34 kDa; TM; hd w/Eβ	Same as *Aβ*	Same as *Aβ*
	Ob	O		Thymic medulla, B cells	Unknown
S	*21-OH*	Steroid 21-hydroxylase	52 kDa	Adrenal gland	Cortisol and aldosterone synthesis
	C4	C4	200 kDa (93 α, 78 β, 33 γ); S	Liver	Complement component
	Slp	Sex-limited protein	200 kDa (105 α, 72 β, 32 γ); S	Liver	Homolog of C4, not functional
	RD	RD	42 kDa	Ubiquitous	Housekeeping function?
	Bf	Factor B	909 kDa (30 Ba, 60 Bb); S	Liver	Alternative complement pathway
	C2	C2	102 kDa; S		Classical complement pathway
D	*B144*	B144	800-nucleotide transcript	B cells, macrophages	Unknown
	TNFα	Tumor necrosis factor	17 kDa; S (and TM?); multimeric	Macrophages	Antitumor activity, cachectin
	TNFβ	Lymphotoxin	25 kDa; S	Activated T lymphocytes	Antitumor activity
	D	D (class I)	45 kDa; TM; hd w/β2M	Virtually all nucleated cells	Same as *K*
	L	L (class I)	45 kDa; TM; hd w/β2M	Virtually all nucleated cells	Same as *K*
	Q4	Qb-1 (class I-like)	41 kDa; S; hd w/β2M	B and T cells	Unknown
	Q5	None (pseudogene)			
	Q6		?	Thymus transcript	Unknown
	Q7	Qa-2, Qa-11 (class I-like)	40 kDa; PI-linked TM and S; hd w/β2M	Day 9–11 embryos, hematopoietic stem cells, activated T cells, liver	Unknown
	Q8/9		40 kDa; TM and S; hd w/β2M	T-cell subsets	Unknown
	Q10	Q10 (class I-like)	40 kDa; S; hd w/β2M	Fetal yolk sac and liver, adult liver	Unknown
TL	*T1*	None (pseudogene)			
	T3		50 kDa; TM; hd w/β2M	T leukemias	Unknown
	T11	None (pseudogene)			
	T18	TL (class I-like)	47 kDa; TM; hd w/β2M	Thymocytes, activated T cells	Unknown
	T22	None (pseudogene)			
	T23	Qa-1 (class I-like)	48 kDa; TM; hd w/β2M	Ubiquitous	Antigen presentation to γ/δ T cells?
	T24		?	Intestinal T lymphocytes and epithelium	Unknown

[a] According to the recently revised *H-2* nomenclature (35).
[b] TM, transmembrane protein; hd w/, heterodimer with; β2M, beta-2 microglobulin (a 12-kDa soluble protein encoded on chromosome 2); S, secreted protein; PI, phosphatidylinositol.

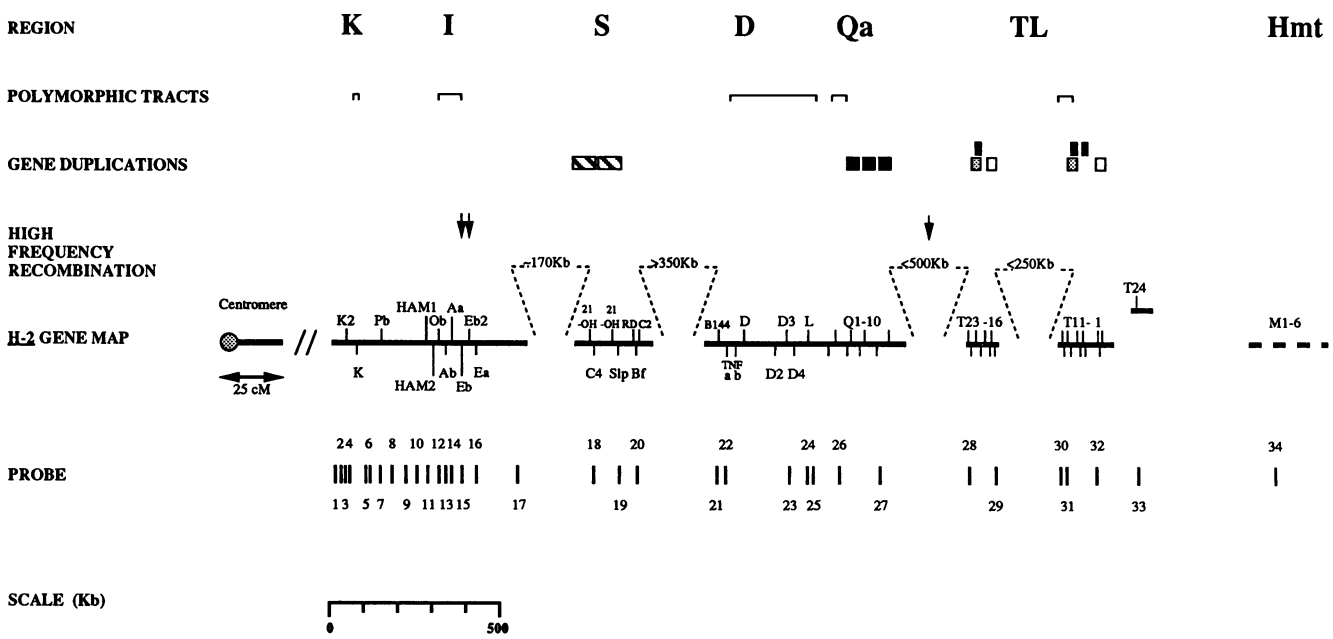

FIG. 1. Genetic map of the MHC of *H-2*^{d} haplotype mice. The positions of probes used in this study, identified in Table 2, are indicated below the gene map. Genes are named according to the recently revised nomenclature (35). Gene positions and approximate distances between cosmid-mapped regions are based on previously published studies (6, 13, 23, 29, 48, 55, 57, 63, 66, 67, 69, 73). The orientation of the two largest *TL* region gene clusters, *T23-16* and *T11-1*, is based on the recombinational analysis (51). The *T24* gene is closely linked to the other *TL* genes, but its precise position relative to *T23-16* and *T11-1* is not known. The dotted line in the *Hmt* region indicates that it has not been mapped by overlapping cosmids, and therefore the extent of this region and the order of genes *M1* to *M6* are not known. Several organizational features of the MHC are noted above the gene map. Brackets indicate tracts of relatively high genetic polymorphism based on restriction fragment length polymorphism analysis and sequence polymorphism in gene coding regions (62). Related chromosomal segments derived from gene duplications are defined by matching bars in the *S* (11), *Qa* (56), and *TL* (23) regions. Arrows mark the locations of relatively high frequency meiotic recombination sites between the MHC of *H-2*^{d} and other inbred strains in the *I* (64, 65) and *Qa-TL* (52, 60a) regions. cM, centimorgans.

region contains >2,000 kb of DNA encoding over 50 well-characterized genes and pseudogenes (Fig. 1). Many DNA probes are available for mapping the relative order of DNA replication in this region. Several contiguous stretches over 400 kb long have been mapped by cosmid walking (40, 63, 66). The *K-I* and *D-Qa* regions are both >600 kb and therefore should each contain at least one replicon. The overall length of >2,000 kb affords opportunities to examine a cluster of replicons and to analyze the relationship between the temporal order of replication and organizational features of chromatin such as G- and R-banding regions. In addition, some MHC genes show tissue-specific regulation (Table 1), permitting an analysis of the relationship between gene transcription and the timing of replication. We were also interested in determining whether the locations of replication origins and the boundaries of replicons correspond to several interesting genetic features of the MHC, including polymorphic sequence tracts and recombination hot spots.

Our data on the relative order of replication provide evidence for several potential replicons in the MHC which coincide in some cases with regions containing related genes. The results also suggest the locations of several potential replication origins and indicate that this extended chromosomal region may contain both symmetric and asymmetric replicons. The earliest-replicating regions in the MHC coincide with actively transcribed genes, whereas the *Hmt* region of the MHC, a region of *H-2* in G-band chromatin, replicates significantly later in S phase.

MATERIALS AND METHODS

Cell culture and BrUdR labeling. Cell lines WEHI-3 (mouse myelomonocyte) and S49.1 (mouse T lymphoma) were obtained from the American Type Culture Collection (Rockville, Md.). The cells were cultured at 1×10^5 to 5×10^5 cells per ml in Dulbecco's modified Eagle's medium containing 10% heat-inactivated fetal bovine serum (FBS). To label replicating DNA, log-phase cells were pulsed with 60 μM bromodeoxyuridine (BrUdR) and 0.5 μCi of [^{3}H]thymidine (6.7 Ci/mmol; NEN) per ml for 1 (S49.1) or 1.5 (WEHI-3) h. The labeled cells were washed three times with cold 1% FBS in phosphate-buffered saline (PBS) with 0.3 mM EDTA and resuspended at a concentration of 2×10^7 cells per ml for centrifugal elutriation.

Centrifugal elutriation and isolation of BrUdR-labeled DNA. A maximum of 2×10^8 cells were loaded into the chamber of a JE-6B elutriator rotor housed in a J-6M centrifuge (Beckman Instruments). The S49.1 cells were sorted at a constant rotor speed of 2,400 rpm by increasing the flow rate of 1% FBS–PBS from 13 to 33 ml/min with a Masterflex Digi-Staltic peristaltic pump (Cole-Parmer Instrument Co.). WEHI-3 cells were elutriated by increasing the pump speed from 15 to 39 ml/min. Fractionated cells were washed twice in PBS and fixed in 70% ethanol. Aliquots of each fraction were resuspended at a final concentration of 10^6 cells per ml in PBS containing 50 mM $MgCl_2$, stained with 20 μg of chromomycin A3 (Sigma) per ml, and analyzed for DNA content on an EPICS 753 flow cytometer (Coulter

Electronics) with an excitation wavelength of 457 λ and a 590/610-λ bandpass collection filter. The average DNA content of each elutriated fraction was determined by integrating the areas under the DNA histograms by using the INTGRA program (Coulter Electronics). On the basis of this analysis, the size-fractionated cells from several elutriation runs were pooled into fractions corresponding to G_1, G_2/M, and four arbitrarily defined fractions of S phase: S1, S2, S3, and S4. The range and mean DNA concentrations of these fractions are as follows: G_1, <2.05C; S1, 2.1 to 2.2C, mean 2.15C; S2, 2.3 to 2.5C, mean 2.4C; S3, 2.6 to 2.9C, mean 2.75C; S4, 3.1 to 3.5C, mean 3.3C; and G_2/M, >3.6C (2C = diploid DNA content). Elutriated fractions with an average DNA content intermediate between the contents of these populations were discarded to minimize overlap as in previous studies using this method (10).

The cells were resuspended in lysis buffer (0.5% sodium dodecyl sulfate [SDS], 200 mM Tris [pH 8.0], 100 mM EDTA, 0.1 mg of proteinase K per ml, 0.1 mg of RNase A per ml) and incubated for 12 to 16 h at 37°C. The DNA was extracted with phenol-chloroform-isoamyl alcohol (25:24:1) and digested with 5 U of *Hin*dIII (100,000 U/ml; New England Biolabs, Inc.) per μg of DNA for 4 h at 37°C. An aliquot of the *Hin*dIII-cleaved DNA was electrophoresed to confirm complete digestion. The BrUdR-labeled DNA (heavy/light [HL]) was isolated on a CsCl gradient formed by centrifugation of 1.725 g of CsCl per ml in a Beckman VTi80 rotor at 55,000 rpm for 48 h at 22°C. The gradient was separated into 36 fractions, and the 5 fractions surrounding and including DNA with a density of 1.74 g/ml (BrUdR-labeled HL DNA) were pooled for electrophoresis.

Southern blot hybridization and quantitation. The DNA concentrations of *Hin*dIII-digested HL fractions from the S1 to S4 cell populations were measured spectrophotometrically and adjusted to 75 μg/ml. Samples (2 μg each) of HL fractions S1 to S4 were loaded into successive wells of a 0.6% agarose-Tris-borate-EDTA minigel and electrophoresed. The gels were then stained in 1 μg of ethidium bromide per ml for 10 min to check for proper separation. Gels were incubated for 4 min in 0.25 M HCl to depurinate the DNA and then subjected to two denaturing washes in 0.5 M NaOH–1.5 M NaCl. DNA was transferred onto Hybond-N or Hybond-N+ nylon hybridization filters (Amersham) by vacuum for 1 h with a MilliBlot-V vacuum transfer apparatus (Millipore). After vacuum transfer, the gels were washed for 5 min in 2× SSC (1× SSC is 0.15 M NaCl plus 0.015 M sodium citrate) and dried at 80°C for 1 h.

The relative replication order of MHC genes and intergenic segments was measured by hybridization with the probes listed in Table 2, corresponding to DNA segments indicated in Fig. 1. Probe fragments were isolated from low-melting-point agarose gels and labeled with 50 μCi of [^{32}P]dCTP (Amersham) by random hexamer primer extension with Klenow polymerase I (New England Biolabs) (22). Unincorporated [^{32}P]dCTP was removed by spin column chromatography.

In preparation for hybridization, filters were washed for 30 min at 65°C in a solution of 0.1× SSPE (15 mM NaCl, 1 mM sodium phosphate [pH 7.4], 0.1 mM EDTA) and 0.1% SDS. Filters were prehybridized for at least 1 h at 65°C in 6× SSC (0.9 M NaCl, 90 mM sodium citrate [pH 7.0])–5× Denhardt's solution (0.1% Ficoll type 400, 0.1% polyvinylpyrrolidone, 0.1% bovine serum albumin)–0.5% SDS–200 μg of salmon sperm DNA per ml. Each filter was hybridized overnight at 42°C with one to three radiolabeled probes at a concentration of 2.5 × 10^6 cpm/ml in 3 ml of 6× SSPE–5× Denhardt's solution–0.5% SDS–50% formamide–200 μg of salmon sperm DNA per ml. Alternatively, some filters were prehybridized and hybridized in a solution of 5× SSC, 25 mM Tris-HCl (pH 7.5), 1.25× Denhardt's solution, 0.125% SDS, 50% formamide, 20 μg of salmon sperm DNA per ml, and 12.5% dextran sulfate. Each filter was washed for 10 min in 2× SSC at 42°C and then subjected to two 12-min washes in 1× SSC–0.1% SDS and one 7-min wash in 0.1× SSC at 65°C. The hybridized filters were wrapped in plastic film and exposed to preflashed X-Omat XAR-5 X-ray film (Kodak) with an intensifying screen at −70°C for 1 to 14 days. The hybridization signals on the fluorograms were quantitated on an Ultrascan laser densitometer (LKB). Blots were stripped for 1 to 2 h with 5 mM Tris-HCl (pH 8)–2 mM EDTA–0.1× Denhardt's solution at 65°C or 1 h in 1% SDS–0.1× SSC, with cooling from 100°C to room temperature. Filters were stripped and reprobed up to six times.

RESULTS

Determination of the relative order of DNA replication in the MHC of elutriated cell lines. Two cell lines were chosen for analysis of the temporal order of DNA replication in the MHC: WEHI-3, a myelomonocytic line, and S49.1, a T-cell lymphoma line. Both cell lines were derived from the BALB/c mouse strain and therefore carry the *d* alleles for all *H-2* genes (36). Cell lines with the *H-2^d* haplotype were chosen because the *H-2^d* chromosomal region has been mapped in detail at the molecular level (5, 11, 13, 23, 40, 47, 63, 66, 67, 73). These particular cell lines were chosen because preliminary flow cytometry experiments with asynchronous WEHI-3 and S49.1 cells revealed an approximately linear correlation between cell size and DNA content (data not shown). This correlation is essential for the effective elutriation of asynchronous cells into discrete subpopulations of S phase. In general, the asynchronous cell population included 30 to 40% S-phase cells prior to elutriation.

The asynchronous cells were pulsed with the higher-density thymidine analog BrUdR for 1 to 1.5 h to label the replicating DNA in each S-phase cell. Elutriation conditions were optimized for the two cell lines to facilitate the size fractionation of the S-phase cells. Elutriated S-phase cells were pooled into four intervals of S phase with progressively higher average DNA content, designated S1 (2.1 to 2.2C), S2 (2.3 to 2.5C), S3 (2.6 to 2.9C), and S4 (3.1 to 3.5C). The elutriated cells with DNA contents intermediate between those of these S intervals were discarded to limit overlap. Figure 2 shows the DNA content distribution of each fraction of elutriated and pooled S49.1 and WEHI-3 cells measured by flow cytometry. The high percentage of cells in G_1 and the small size difference between G_1 and early S cells resulted in a considerable contamination of the early S-phase fractions with G_1 cells. Prolonged elutriation at low pump speeds did not completely remove the G_1 cells from the S1 and S2 fractions.

DNA which replicated during a particular S interval contained the density label BrUdR on one of the strands (HL) and therefore could be separated by isopycnic centrifugation from the DNA which did not replicate during the same interval. As expected, there was no recoverable HL DNA in the G_1 cells, and therefore any contaminating G_1 cells in S-phase fractions should not cause measurable contamination of the gradient-purified replicating DNA. Thus, the different levels of contamination of G_1 cells in the S-phase fractions of the two cell lines will not affect the data.

TABLE 2. Locations and sources of MHC probes used in replication analysis

Region	Probe	Location[a]	Source[b]	Size (kb)	Restriction endonuclease fragment	Reference[c]
K-Ia	1	45c*K2*	cos II 6.3	3.4	*Sal*I-*Bss*HII	62
	2	20c *K2*	cos 3-6-3	1.8	*Pst*I	1
	3	15c *K2*	cos 3-6-3	1.8	*Eco*RI	1
	4	5c *K2*	cos 17.1	2.6	*Xho*I-*Nru*I	73
	5	25t *K*	cos 3-1-2	4.9	*Bam*HI	1
	6	40t *K*	cos 3-1-2	7.1	*Bam*HI	1
	7	5c *Pb*	cos II 10.6	2.2	*Kpn*I	64
	8	5t *Pb*	cos II 10.6	2.6	*Kpn*I-*Sal*I	64
	9	45t *Pb*	cos II 5.22	1.6	*Bss*HII	64
	10	20c *HAM1*	cos II 5.10	1.2	*Sal*I-*Xho*I	64
	11	*HAM1*	cos II 5.10	2.0	*Sma*I	64
	12	*Ob*	pC17	1.5	*Hin*dIII-*Pvu*II	NR
	13	*Ab*	*A*β cDNA	0.8	*Pst*I	20
	14	*Aa*	pBal17	0.8	*Pvu*II-*Bst*EII	15
	15	*Eb*	pEB10	2.0	*Eco*RI	46
	16	*Ea*	pEAC11	0.9	*Eco*RI-*Tth*III	45
	17	110t *Ea*	cos 61.1	5.6	*Eco*RI	62
S	18	*C4*	pMLC4/w7-2	0.5	*Pst*I	50
	19	*Slp*	pSlp/w7-1	0.6	*Pst*I	49
	20	*C2*	pC2M1	0.9	*Pst*I	21
D-Qa	21	*B144*	*B144* cDNA	0.4	*Bam*HI	68
	22	*TNF*	MuTNF cDNA	1.1	*Eco*RI	53
	23	10t *D3*	cos 50.2	2.0	*Sma*I	73
	24	5c *L*	p14913-1	0.6	*Bgl*II	NR
	25	10t *L*	cos 59.2	3.1	*Sau*3A	73
	26	*Q1*	pQ1	0.6	*Eco*RI-*Hin*dIII	NR
	27	10t *Q8/9*	cos 46.1	2.9	*Cla*I-*Sma*I	57
TL	28	t *T21*	cos 47.1	2.6	*Hpa*I-*Xho*I	73
	29	t *T16*	cos 22.1	2.0	*Bam*HI	73
	30	5c *T11*	cos 12.2	2.2	*Eco*RI	73
	31	*T10*	pT9/17	0.7	*Eco*RI-*Hin*dIII	NR
	32	c *T3*	cos 49.1	3.0	*Hpa*I	73
	33	*T24*	pMT21	0.7	*Eco*RI-*Hin*dIII	NR
Hmt	34	*M1*	pP1.4	1.2	*Pst*I	60
Centromeres	35	Repetitive	pSat1	0.5	*Ava*II	54

[a] Locations of probes derived from intergenic regions are referenced in kilobases from the nearest known gene or pseudogene: c, centromeric; t, telomeric (e.g., probe 1 was derived from a 3.4-kb *Sal*I-*Bss*HII intergenic fragment of cosmid II 6.3 located 45 kb centromeric of pseudogene *K2*). The satellite DNA probe pSat1 hybridizes to repetitive sequences in the vicinity of centromeres.

[b] cos, cosmid; MuTNF, murine tumor necrosis factor.

[c] NR, not referenced. Information provided by Werner Mayer (Max Planck Institute) for probe 12, by Suzanne Watts in the laboratory of R. Goodenow (University of California, Berkeley) for probes 24 and 26, and by Kurt Brorson in the laboratory of L. Hood (California Institute of Technology) for probes 31 and 33.

Equal quantities of *Hin*dIII-digested HL DNA from each fraction of S phase were electrophoresed, blotted, and probed to determine the timing of replication of various MHC genes and intergenic segments. Sample fluorograms from WEHI-3 and S49.1 HL DNA are shown in Fig. 3. Some probes, such as the *Aa* probe 14 (Fig. 3B), hybridized to a single *Hin*dIII fragment. In other cases, a hybridizing sequence contained a *Hin*dIII site and therefore yielded two bands (e.g., Fig. 3C, bands 5 and 9). The MHC contains several gene duplications (23, 56, 67), and therefore some probes hybridized to multiple bands. This was a potential problem in the analysis of the *Qa* and *TL* regions. Several of the probes from the *Qa* and *TL* regions cross-hybridized to identical-size *Hin*dIII fragments or to fragments too close in size to be distinguished by the laser densitometer. To identify the source of each cross-hybridizing band, we hybridized each probe from the *Qa* and *TL* regions to a panel of *Hin*dIII-digested cosmids spanning these regions and mapped the *Hin*dIII sites in these cosmids (data not shown). Only the hybridizing bands corresponding to a single identified DNA segment were used. For example, probe 29 isolated from an intergenic region 5′ of the *T16* gene cross-hybridizes to DNA 5′ of *T1* and 3′ of *T11*. *Hin*dIII fragments from 5′ *T1* and 3′ *T10* are both 2.0 kb (Fig. 3C, band 8). Because this 2.0-kb band represents the replicating DNA from two separate chromosomal locations, it was not used in the analysis of temporal replication order in the *TL* region. The 3.2-kb band (Fig. 3C, band 5) and 1.5-kb band (Fig. 3C, band 9) were unique to the 5′ *T16* sequence, and the cross-hybridizing 11-kb band (Fig. 3C, band 2) was unique to 5′ *T1*. Therefore, these bands were used for the replication analysis.

The intensities of the hybridizing bands for the four S-phase fractions on each fluorogram were quantitated by laser densitometry. To determine the relative time period in S phase during which a particular DNA segment is replicated, the band intensity of hybridization to S1 HL DNA was normalized as the ratio of S1-phase hybridization relative to the total band intensities for the sum of lanes S1 to S4: (S1/S1 + S2 + S3 + S4) × 100. We refer to this normalized value as the relative hybridization value for S1 (RHVS1). The RHVS1 does not represent the precise time during S phase in which a DNA segment replicates, but comparison of the RHVS1 of various DNA segments can be used to

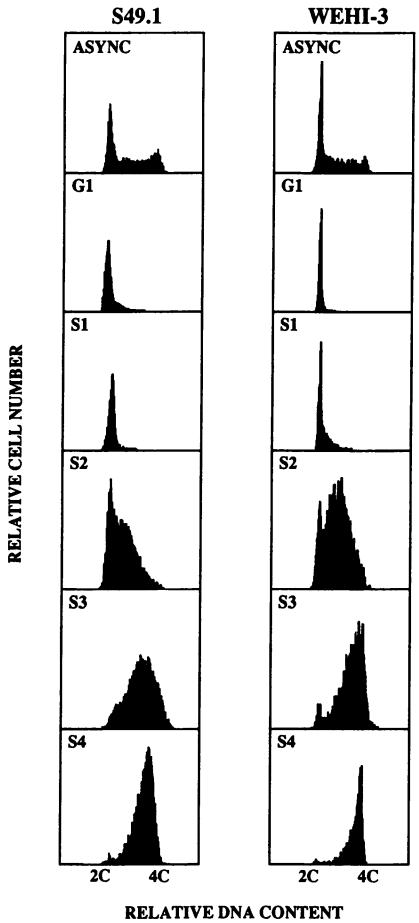

FIG. 2. Fluorescence histograms of DNA content in asynchronous and elutriated S49.1 and WEHI-3 cells. Logarithmically growing cells were fractionated according to size by centrifugal elutriation. To measure the cell cycle distribution of asynchronous and elutriated populations, aliquots of cells were fixed in ethanol, stained with chromomycin A3, and analyzed for DNA content by flow cytometry. Fractionated cells from several elutriations were pooled into four subintervals of S phase. The histograms of asynchronous cells and subfractions S1 to S4 are plotted with relative cell number (ordinate) against DNA content measured by chromomycin A3 staining (abscissa).

assign a relative temporal order of DNA replication. Thus, the higher the RHVS1, the earlier a sequence is replicated in S phase.

The fluorograms in Fig. 3 reveal variation in the relative hybridization of different MHC probes to the subfractions of S1 to S4 replicating DNA. The *T10* probe 31 hybridized primarily to S49.1 DNA replicating during S1, with RHVS1 values of 61.3 and 59.5 for bands 1 and 2, respectively (Fig. 3D). In contrast, replication in the *Hmt* region gene *M1* of S49.1 occurs predominantly during S2, with an RHVS1 value of 22.3 (Fig. 3E, band 1). With probe 29, a weakly cross-hybridizing DNA segment of unknown chromosomal location appeared predominantly in the S4 lane of replicating WEHI-3 DNA, with an RHVS1 value of <2.0 (Fig. 3C, band 1). Overall, quantitation of the hybridizing bands yielded RHVS1s in the range of 29.4 to 69.0 within the *H-2* region of S49.1 cells and of 34.8 to 67.3 within the *H-2* region of WEHI-3 cells. Figure 4A presents examples of the normalized hybridization values from several probes used to screen replicating S49.1 DNA. The histograms show that none of the genes tested replicate solely in a single portion of S phase as defined by the elutriated fractions. This is not surprising given the unavoidable overlap of the elutriated fractions. The probes shown in Fig. 4A differ in the segment of S phase when replication peaks, with the peaks in S1 for probes 31 (*T10*) and 3 (3′ *K2*), S2 for probes 17 (3′ *Ea*) and 34 (*Mb-1*), and S4 for probe 35 (satellite DNA). Probe 35 hybridizes with an A+T-rich, centromere-associated set of repetitive sequences comprising 5 to 10% of total genomic DNA. Centromere-associated satellite sequences replicate late in the S phase of human cells (26). Figure 4A shows that these mouse satellite sequences also replicate late in S phase. In contrast, most *H-2* region genes replicate relatively early in S phase. In several regions of *H-2*, there was a marked gradient in the RHVS1 of hybridizing sequences. For example, Fig. 4B shows the distribution of normalized hybridization values obtained with S49.1 T-lymphoma DNA for several probes within a 230-kb portion of the *I* region, spanning from *Ob* to 115 kb telomeric of *Ea*. Within this segment of the *I* region, the RHVS1 of the sequences hybridizing to the probes decreases proportionally to its distance from the *Ob* gene (see below). Therefore, the order of replication within this region is *Ob-Ab-Aa-Ea*.

Relative order of DNA replication in the *K* and *I* regions. The RHVS1s for all of the unique bands hybridizing to the 34 *H-2* probes in this study were plotted against position in the *H-2* complex to determine the temporal order of replication and to identify possible replicon boundaries. Figure 5 shows the relationship between the relative time of replication, represented by the RHVS1, and the position of the hybridizing sequences within the *K* and *I* regions of the *H-2* complex. To minimize variations in RHVS1s due to differences in the amount of DNA loaded in each lane or in transfer efficiency, hybridizations with *K* region probes 1 to 9 were performed by stripping and reprobing the same filter, while *I* region probes 10 to 17 were hybridized to a separate filter. Several probes to the *K* and *I* regions demonstrate the reproducibility of the RHVS1s. For example, probes 5 and 6 hybridize to opposite ends of the same 24-kb *Hin*dIII segment of $H\text{-}2^d$ genomic DNA. Hybridization to S49.1 HL DNA yielded nearly identical RHVS1s of 56.5 and 55.0 for probes 5 and 6, respectively. The *Ab* cDNA probe 13 hybridizes to two adjacent *Hin*dIII fragments of 2.7 and 1.7 kb which contain *Ab* exons. This probe hybridizes to these two restriction fragments in WEHI-3 HL DNA with average RHVS1s of 57.1 (5′ fragment) and 55.8 (3′ fragment), demonstrating a close correlation in the results obtained for these small adjacent segments.

The data from both cell lines are consistent with the *I* region replicating as part of a single replicon (see Discussion). As the histograms in Fig. 4B demonstrated, the RHVS1s of probes in the *I* region of S49.1 cells decrease from 61.8 to 34.7 over the 230 kb between probes 12 and 17 (Fig. 5, open circles). A similar gradient of RHVS1 versus distance was found by probing several blots of WEHI-3 S1 to S4 HL DNA with probes 12 to 17 (Fig. 5, closed circles). Linear regression analysis of this region produces a slope of −10.3 RHVS1/100 kb and $r = -0.951$ in S49.1 cells and a slope of −9.5 RHVS1/100 kb and $r = -0.878$ in WEHI-3 cells.

Another RHVS1 gradient occurs in a chromosomal segment telomeric to the *K* gene. The earliest replication in the *K* region of S49.1 cells (Fig. 5, open circles) occurs in the vicinity of the *K2* and *b-c* genes, with lower RHVS1s in both the centromeric and telomeric directions. Linear regression

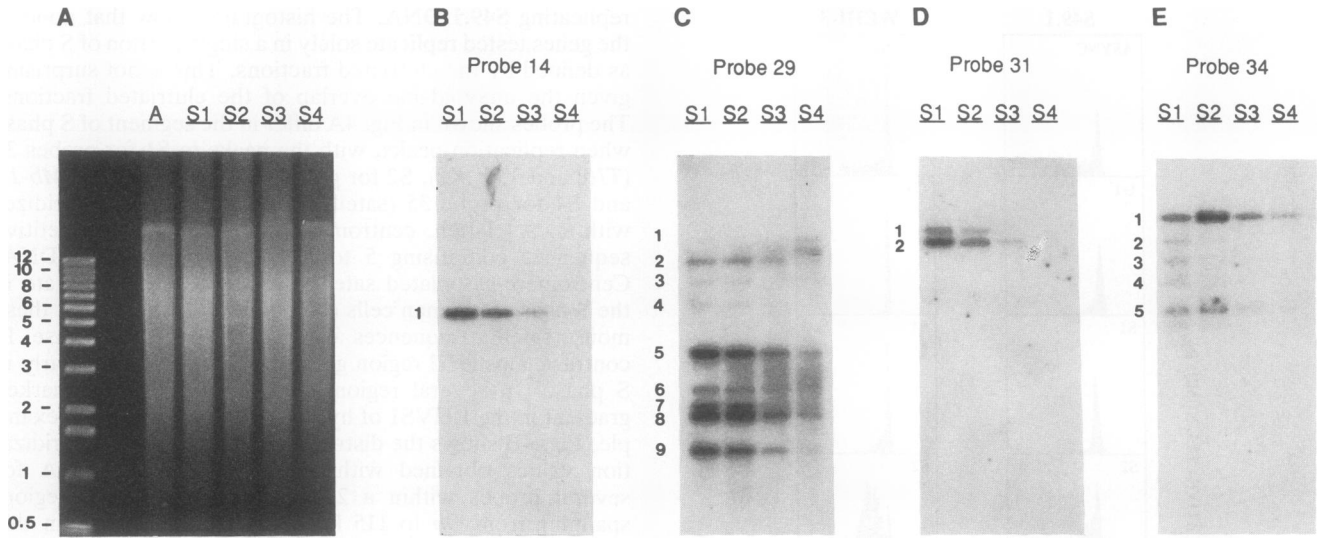

FIG. 3. Sample autoradiograms demonstrating the distribution of replication during S-phase intervals S1 to S4 of several MHC sequences. DNA from each elutriated interval of S phase was digested with *Hin*dIII, and the DNA which replicated during each S-phase interval (BrUdR-labeled HL hybrid) was separated from the nonreplicated lighter DNA light/light) on cesium gradients. Equal quantities of HL DNA (2.25 μg per lane) from fractions S1 to S4 were electrophoresed in agarose minigels, blotted, and probed. (A) Representative gel stained with ethidium bromide, showing equal quantities of WEHI-3 HL DNA from an asynchronous population (lane A) and elutriated S-phase intervals S1 to S4. A 1-kb DNA ladder (GIBCO-BRL) with bands in the range of 0.5 to 12.0 kb was loaded in the left lane to provide calibration of the gel. (B) Fluorogram of WEHI-3 HL DNA hybridized with *Aa* probe 14. (C) Fluorogram of WEHI-3 HL DNA hybridized with *TL* region probe 29, derived from an intergenic segment telomeric to *T16*. Several bands were identified by hybridization to *Hin*dIII-digested *TL* region cosmids (data not shown). Bands 5 and 9 represent *Hin*dIII fragments which overlap the 2.0-kb *Bam*HI probe sequence telomeric to *T16*. Bands 2 and 6 are cross-hybridizing sequences telomeric to *T1*. Band 8 results from two identical size *Hin*dIII fragments located telomeric to genes *T1* and *T11*. The sources of cross-hybridizing bands 1, 3, 4, and 6 could not be identified. (D) Fluorograms of S49.1 HL DNA hybridized with *TL* region probe 31. Bands 1 and 2 represent hybridization to *Hin*dIII fragments of genes *T23* and *T10*, respectively. (E) Fluorogram of S49.1 HL DNA hybridized with *Hmt* probe 34. Band 1 results from hybridization to gene *M1*; the sources of bands 2 to 5 are unidentified.

analysis of the S49.1 RHVS1s from probes 5 to 8 and 10 yields a slope of −6.2 RHVS1/100 kb and $r = 0.960$. The RHVS1s of WEHI-3 HL DNA hybridized with probes 7 and 9 also fall on this temporal gradient. Therefore, both cell lines show replication apparently proceeding telomerically from a position centromeric to gene *e*. The scatter of the data obtained with probes 1 to 4 and the relatively short distance covered by these probes preclude a definitive assignment of replication order in this centromeric end of the *K* region.

Relative order of DNA replication in the *S*, *D*, and *Qa* regions. The relationship between replication timing in WEHI-3 cells and gene position in the *S*, *D*, and *Qa* regions of the *H-2* complex is plotted in Fig. 6. The *S* region of the *H-2* complex includes about 300 kb linked by cosmids and contains a tandem duplication indicated by the striped bar in Fig. 6. In WEHI-3 cells, the *Slp* probe 19 hybridizes to the *Slp* gene with an RHVS1 of 61.9. This is the highest RHVS1 in the *S* region and is comparable to the highest RHVS1s in the *K* and *I* regions. Probe 19 cross-hybridizes to a related sequence in this duplication encoding the *C4* gene. The *Slp* and *C4* *Hin*dIII fragments which hybridize to probe 19 are 23 and 5 kb, respectively (49). Therefore, probe 19 can measure the relative replication timing of both of these *S* region genes. The RHVS1 of the *C4* cross-hybridizing band is 52.0. Stripping the blot and hybridizing it with probe 18, which hybridizes only to the *C4* gene, yielded a 5-kb hybridizing band with an RHVS1 of 50.4. Thus, the RHVS1s of *C4* DNA determined by two cross-hybridizing probes are in very close agreement. The difference between the RHVS1s of the *Slp* and *C4* genes measured by probe 19 is 9.9 over a distance of 90 kb. This slope of 11.0 RHVS1/100 kb is comparable to the change in RHVS1 measured in the *I* replicon. The *C2* gene in the telomeric portion of the S region hybridizes to probe 20 with a RHVS1 of 53.4, a ΔRHVS1 between *slp* and *C2* of 9.6 RHVS1/100 kb.

The *D* and *Qa* regions of the *H-2* complex span more than 600 kb of contiguous DNA, a chromosomal segment equivalent in size to the *K* and *I* regions. Probes which hybridized with sequences in the vicinity of the *B144*, *TNF*, *D*, and *L* genes of WEHI-3 HL DNA had the highest RHVS1s in these regions, comparable to the highest RHVS1s in the *K*, *I*, and *S* regions. The *Qa* region contains three gene duplications (Fig. 6, solid bars) which complicate the hybridization analysis required to determine the replication order. Probe 27 hybridizes to intragenic sequences between *Q5* and *Q6*, *Q7* and *Q8/9*, and *Q8/9* and *Q10*. The *Hin*dIII sites in these three segments are nearly identical, generating hybridization bands of 9.5, 8.3, 6.2, and 0.9 kb (56; confirmed by our cosmid mapping). The 6.2- and 0.9-kb bands are common to all three segments and therefore cannot be used to analyze the replication order of this gene region. The presence of an extra *Hin*dIII site in the *Q7-Q8/9* segment produces an 8.3-kb hybridizing band which is unique to this segment. Therefore, this 8.3-kb band from probe 27 can be used in the mapping of *Qa* replication order.

The position of replication gradient(s) in the *D* and *Qa* regions is ambiguous. Linear regression analysis of all *D* and *Qa* region RHVS1 data yields an *r* value of 0.932 and a slope of −4.8 RHVS1/100 kb. This slope is significantly smaller than the slopes of replicons in the *K* and *I* regions. Alternatively, a temporal gradient of −7.3 RHVS1/100 kb is derived for the segment between the *D* and *L* genes hybridized with

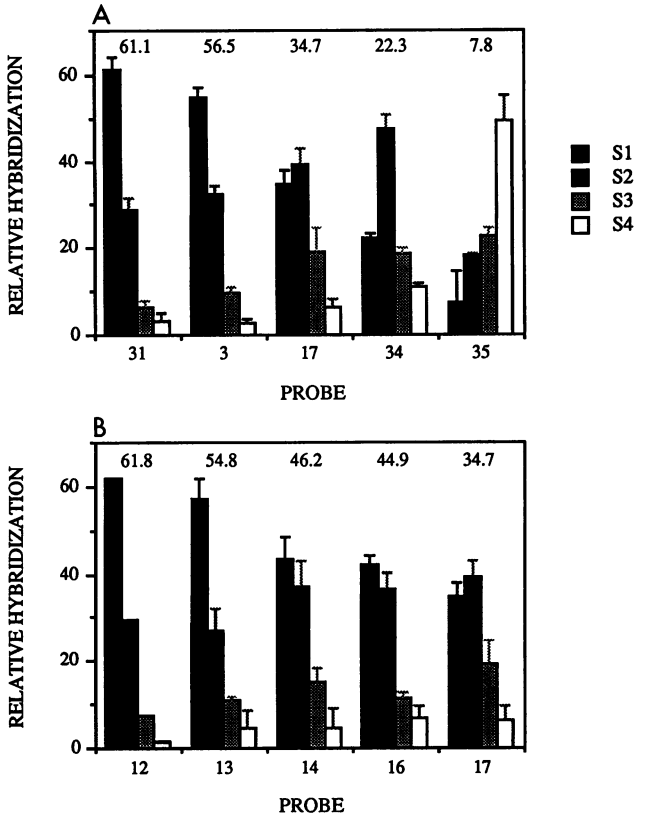

FIG. 4. Relative hybridization of MHC and satellite DNA probes to replicating HL DNA from S-phase intervals. Fluorograms were quantitated by laser densitometry, and the band intensity for each lane was normalized as the proportion of hybridization (×100) relative to the total band intensity for the sum of lanes S1 to S4, essentially the RHVS1 for each S-phase fraction. The RHVS1 values ([S1/S1 + S2 + S3 + S4] × 100) for the probes are listed above the bars. Error bars indicate the standard deviation of multiple exposures and scans. (A) Results with selected probes hybridizing preferentially to S49.1 HL DNA from S1 to S4, including probes from MHC regions *TL* (probe 31), *K* (probe 3), *I* (probe 17), and *Hmt* (probe 34), and from satellite DNA (probe 35); (B) gradient of relative hybridization in the *I* region of S49.1 HL DNA with probes to *Ob* (probe 12), *Ab* (probe 13), *Aa* (probe 14), *Ea* (probe 16), and region telomeric to *Ea* (probe 17).

probe 24 (5′ *L*, with cross-hybridization to 5′ *D*), probe 26, and probe 23 (3′ *D3*). A similar gradient of ΔRHVS1 of −9.3/100 kb occurs between probe 25 (telomeric to *L*) and probe 27 (between *Q7* and *Q8/9*) (Fig. 6, short dashes). These slopes are similar to those obtained for the temporal gradients measured in the *K* and *I* regions.

Relative order of DNA replication in the *TL* and *Hmt* regions. Measurements of relative replication order in the telomeric regions of the *H-2* complex, *TL* and *Hmt*, are summarized in Fig. 7. The *TL* region contains several related segments apparently derived from gene duplication (23), indicated by patterned bars above the gene map. As a result of these duplications, most *TL* probes yielded complex hybridization patterns (e.g., Fig. 3C). In our analysis, only bands shown by cosmid mapping to represent a single identified *Hin*dIII DNA segment were used. However, we cannot eliminate the possibility that similar-size cross-hybridizing sequences exist in the unmapped regions between *D* and *TL*, between *T16* and *T11*, telomeric to *T1*, or on either side of *T24*.

Figure 7 shows significant differences between the RHVS1s of *TL* probes hybridizing to replicating S49.1 and WEHI-3 DNA, in contrast to the similar RHVS1s obtained with the two cell lines in the *K* and *I* regions (Fig. 5). The RHVS1s of S49.1 *TL* region DNA are generally 20 to 30% higher than those of the equivalent regions in WEHI-3 replicating DNA. This finding suggests that the S49.1 *TL* region DNA replicates relatively earlier in S phase than does WEHI-3 *TL* DNA.

The S49.1 T lymphoma expresses TL proteins (32), whereas monocytes and macrophages such as WEHI-3 do not. Northern (RNA) blot analyses of T lymphocytes and T-lymphoma cell lines have shown active transcription of *TL* region genes *T3*, *T18*, *T23*, and *T24* (Table 1). Therefore, the temporal differences in *TL* region replication might be related to transcription. The RHVS1s in the vicinity of S49.1 genes *T18* (probes 26 and 30) and *T3* (probes 23 and 32) are comparable to the RHVS1s around other transcribed genes, including *K*, *HAM*1, *B*144, *D*, and *L* (Fig. 5 and 6).

The *Hmt* region (containing gene *M1*) is the most telomeric and least characterized portion of the *H-2* complex. Recombination analysis estimates a distance of approximately 0.1 centimorgan between *TL* and *Hmt* (55). Hybridization of S49.1 HL DNA with the *M1* probe 34 yielded an RHVS1 of 22.3%, the lowest value of any *H-2* DNA segment; hence, this is the latest-replicating segment.

DISCUSSION

Previous studies demonstrated that mammalian DNA is synthesized in a regulated temporal order and that the timing of replication in a given cell type is consistent over many rounds of mitosis. We have mapped the temporal order of DNA synthesis in the mouse *H-2* MHC to define the organization of replicons in an extended chromosomal region and to determine whether the organization of these replicons coincides with recombinational hot spots, polymorphic sequence tracts, or clusters of related genes. The approach of combining BrUdR density labeling of nascent DNA and centrifugal elutriation to fractionate S-phase cells to determine the timing of DNA replication has previously been applied to measuring the temporal order of replication in smaller gene regions such as the globin and IgH regions (7, 10). The advantage of this technique is it allows the study of replication in an unamplified gene region in an asynchronous cell population. Transcriptionally active chromosomal regions tend to replicate early in S phase (17, 24, 30). Therefore, we deliberately divided S phase into progressively wider fractions (S1, 2.1 to 2.2C; S2, 2.3 to 2.5C; S3, 2.6 to 2.9C; and S4, 3.1 to 3.5C) to increase the resolution for detecting early temporal differences in replication. Because fractions S1 to S4 were not equal portions of S phase, the distribution of hybridization intensities obtained with the S1 to S4 HL DNA cannot be used to define the precise time at which the probed DNA segment replicates. However, a comparison of the relative hybridization intensity patterns of linked DNA sequences clearly showed a temporal order of replication in several regions of the *H-2* complex, suggesting progressional DNA synthesis within a replicon. While it is possible that this temporal order reflects the sequential initiation of many closely spaced replication origins, we feel that this explanation is unlikely in light of fiber autoradiographic studies of the distribution of mammalian replication bubbles. Instead, we believe that each temporal gradient identified represents the position of a replicon with initiation

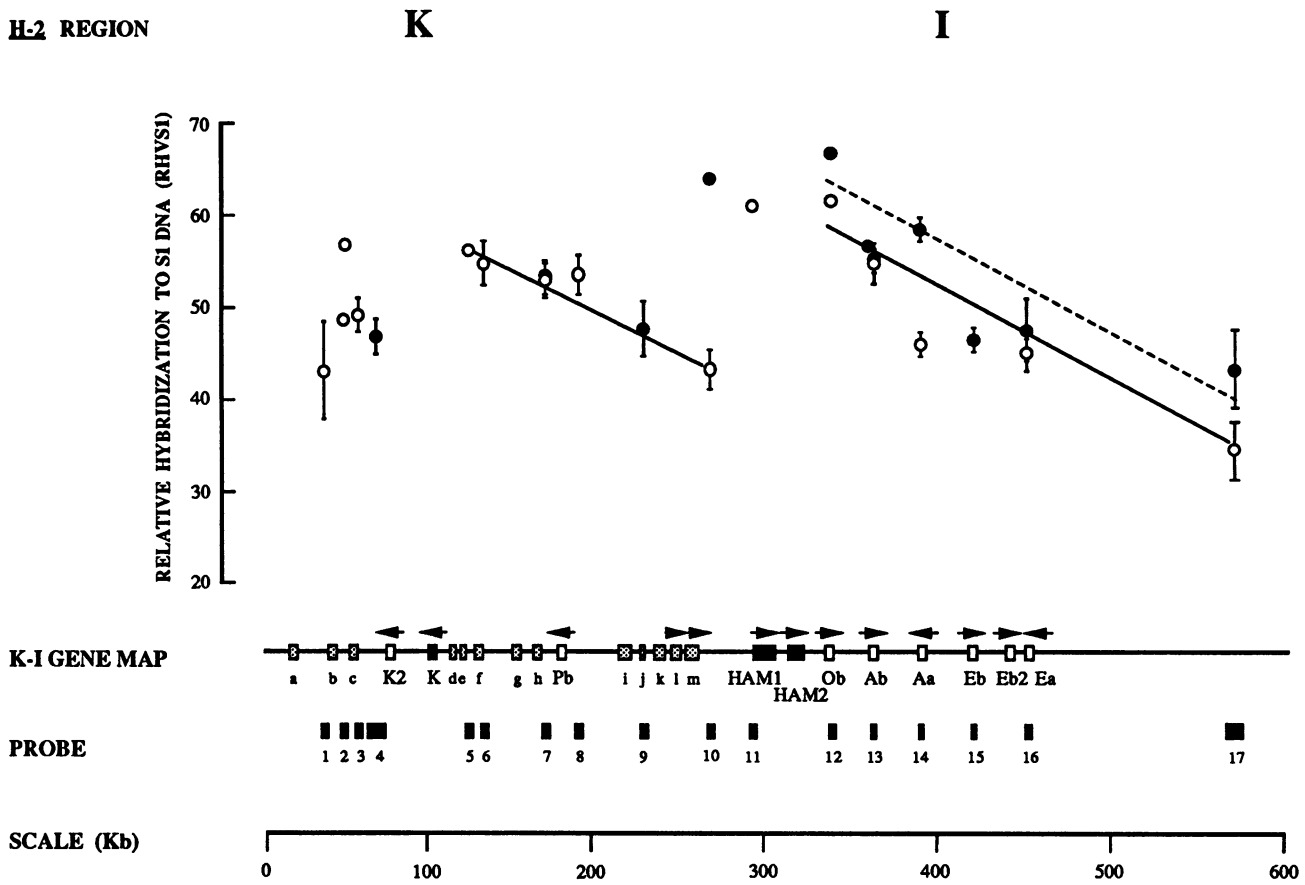

FIG. 5. Timing of replication in the *K* and *I* regions of the MHC. Relative hybridization values of *K* and *I* region probes to the S1 interval HL DNA from S49.1 (open circles) and WEHI-3 (closed circles) cells are plotted against the map position of the hybridizing sequences. Bars indicate the standard deviation of RHVS1 derived from multiple fluorograms and densitometry measurements. The lines indicating the temporal gradients which suggest the positions of replicons are based on linear regression analysis (S49.1, solid lines; WEHI-3, dashed lines). Constitutively transcribed genes are indicated by black boxes in the *K-I* gene map. Nontranscribed genes are indicated by unfilled boxes. Poorly characterized genes and pseudogenes are indicated by stippled boxes as follows: *a* (*KE1*), *b* (*KE2*), *c* (*KE3*), *f* (*KE4*), *g* (*KE5*) (1), *d* (*RING1*), *e* (*RING2*), *h* (*COL11A2*) (29), *i* (*4.24A*), *j* (*4.24F*), *k* (*MA*), *l* (*Mb2*), and *m* (*Mb1*) (13). Gene *i* (*4.24A*) is variably expressed in WEHI-3 cells; genes *k* (*MA*), and *l* (*Mb2*) and/or *m* (*Mb1*) are expressed in WEHI-3 cells at low levels (13). Gene *g* (*KE5*) is expressed in mature macrophages (1), but its status in WEHI-3 and S49.1 cells is unknown. Arrows over the genes indicate the direction of transcription.

of DNA synthesis at a single replication origin, especially for regions in which we have multiple, closely spaced probe-hybridizing sequences (such as the *K* and *I* regions). Regions that do not show a gradient of replication or have more loosely spaced probe-hybridizing regions may initiate replication at several closely spaced origins or randomly within that defined region.

Fiber autoradiography of unidentified replicating DNA in higher eukaryotes has revealed a general replicon size range of 50 to 330 kb (19). The predicted replicon sizes of the limited number of defined mammalian gene regions studied to date fall within this range. The IgH complex replicates as a single unit in non-B cells, with a replicon size of >300 kb (7). This region has not been cloned telomeric of the *Cα* locus, so the location of the replication origin, the size of the replicon, and whether or not it is bidirectional are unknown. In our studies, the *I* region, including the *HAM1-Ea* interval, formed the largest and best-defined apparent replicon in the *H-2* complex. The data suggest that the origin of replication for the *I* region replicon is in the vicinity of, or just centromeric to, the *HAM1* and *HAM2* genes. On the basis of the temporal order of replication, this replicon is >230 kb (Fig. 5). The termination point of this replicon telomeric to *Ea* could not be determined because the gap between the *I* and *S* regions has not been cloned in the mouse. The maximum telomeric extent of this replicon can be calculated on the basis of the pulsed-field gel electrophoresis estimation of ~170 kb between the *I* and *S* regions (48) and the observation that the RHVS1 of the *C4* gene in the centromeric portion of the *S* region is significantly higher than the RHVS1 of probe 17 in the telomeric portion of the *I* region. Therefore, the *I* region replicon probably does not include *C4* and thus should have a maximum size of 450 kb.

The centromeric boundary of this replicon appears to be located at the sharp temporal discontinuity between the sequences hybridizing to probes 9 and 10 (WEHI-3) or to probes 10 and 11 (S49.1) (Fig. 5). In both cell lines, these probe combinations define the boundaries of the *K* and *I* replicons within 25 kb. This apparent shift in boundaries is based on only one probe and therefore should not be overemphasized until confirmed with other probes. The data do not distinguish between the possibilities that this replicon is unidirectional or strongly asymmetric. Fiber autoradiography has shown that up to 10% of the replicons in higher

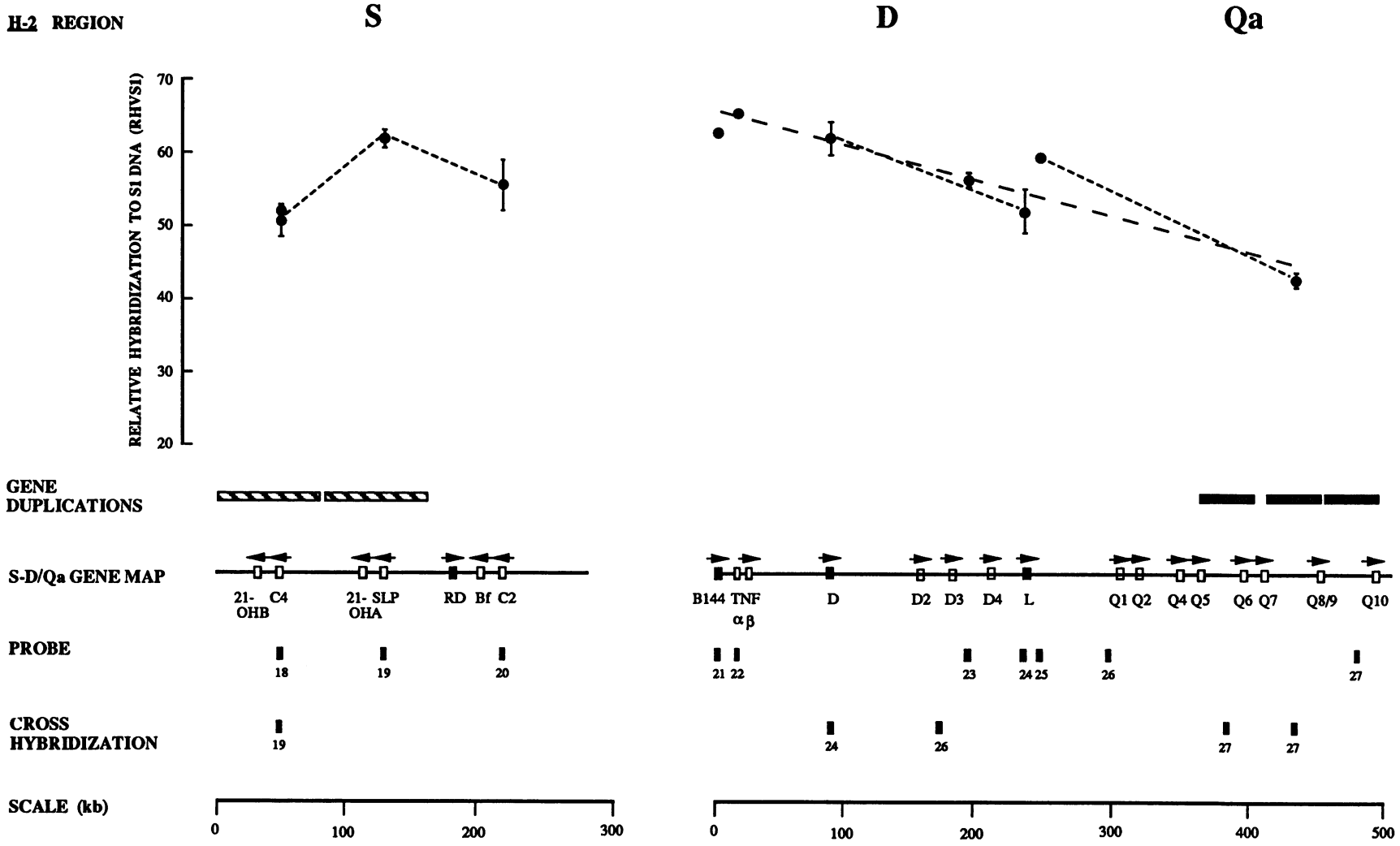

FIG. 6. Timing of replication in the *S* and *D-Qa* regions of the MHC. Relative hybridization values of *S* and *D-Qa* region probes to S1 interval HL DNA from elutriated WEHI-3 cells are plotted against map position. The locations of cross-hybridizing sequences which could be distinguished by unique *Hin*dIII fragment size are listed below the probe locations. Black bars in the telomeric portion of the *Qa* region indicate three blocks of related sequences apparently derived from gene duplications (56). An unrelated gene duplication in the *S* region is indicated by striped bars (11). Genes which are probably transcribed in the WEHI-3 cell line are indicated by black boxes. Two possible interpretations of the temporal order of replication in the *D* and *Qa* regions are indicated by short and long dashes.

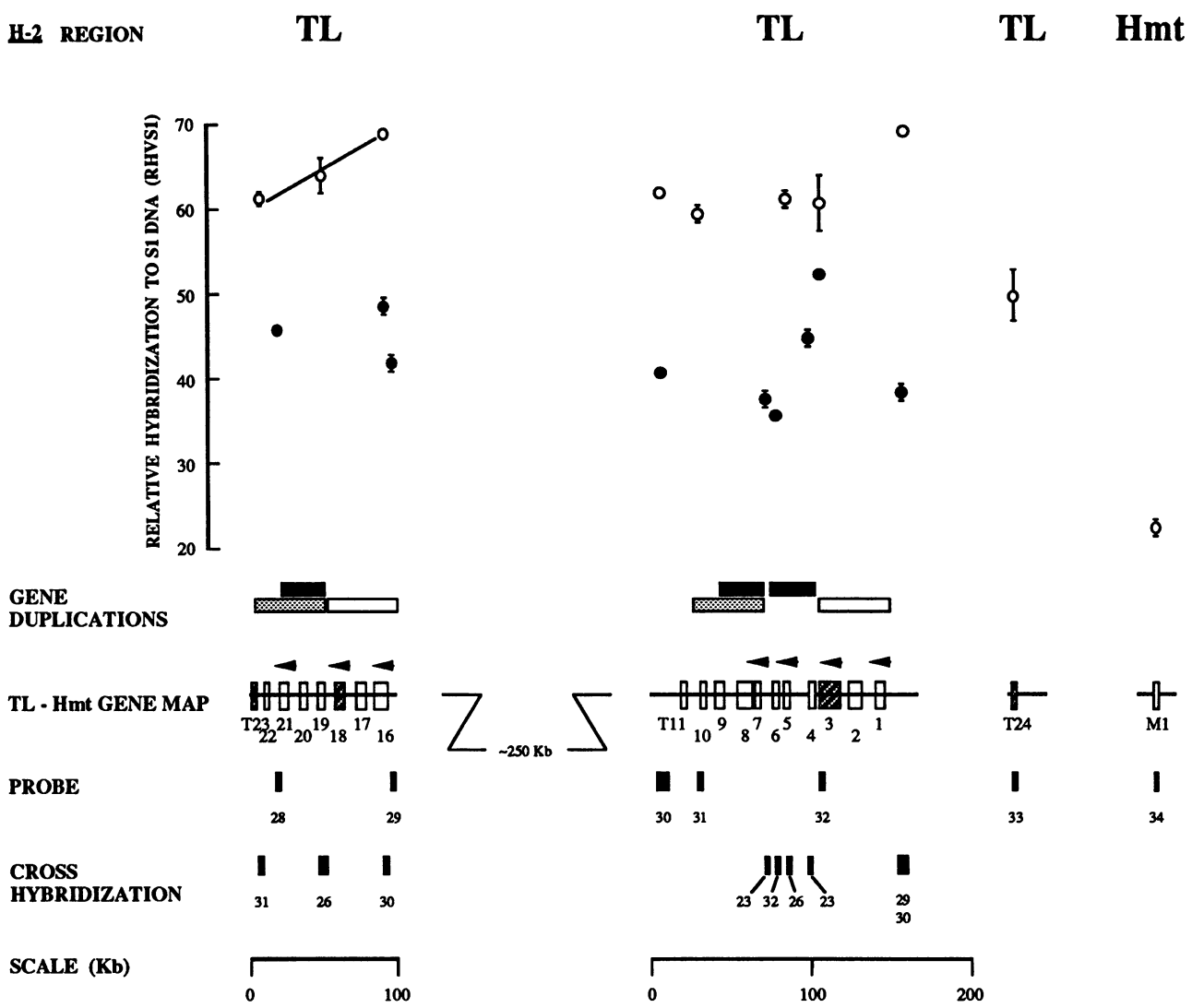

FIG. 7. Timing of replication in the *TL* and *Hmt* regions of the MHC. Relative hybridization values of *TL* and *Hmt* region probes to S1 interval HL DNA from elutriated S49.1 (open circles) and WEHI-3 (closed circles) cells are plotted against map position. The positions of *Hin*dIII fragments of unique size which hybridize with probes from the *TL* or *D/Qa* region are listed below the probe locations. On the basis of expression patterns in thymocytes, genes *T18*, *T3*, *T23*, and *T24* may be transcriptionally active in S49.1 cells (indicated by cross-hatching). The positions of three blocks of related sequences apparently derived from gene duplications (23) are indicated above the gene map by white, black, and stippled bars. The lines indicating the temporal gradient which suggest the positions of replicons are based on linear regression analysis (S49.1, solid line; WEHI-3, dashed line).

eukaryotes are unidirectional (19). Replication of the rRNA genes in many eukaryotes is almost completely unidirectional and proceeds in the same direction as does transcription (19). Several groups have suggested that the steric constraints of replication and transcription complexes force replication to follow the direction of transcription. Replication in the *I* region appears to initiate in the vicinity of the *HAM1* and *HAM2* genes, which are transcribed in WEHI-3 cells (47) and most other nucleated cells (46a). Therefore, the activities of these genes may play a role in dictating the direction of replication in the *I* region replicon.

Both S49.1 and WEHI-3 *I* region DNA had a ΔRHVS1 of approximately −10/100 kb. Similar gradients in the temporal order of replication suggest the location of other replicons in the *H-2* complex. A replication order gradient with a similar slope appears to include part of the *K* region between sequences corresponding to probes 5 and 10 (S49.1) (Fig. 5). The data from probes 1 to 4 do not fit a trend indicating bidirectional replication from an origin near the *K* gene. Temporal mapping centromeric to probe 1 may prove difficult because of repetitive sequences in this region (2a).

Measurements of replication in the *S* region of WEHI-3 cells suggest bidirectional replication initiating in the vicinity of *Slp* (Fig. 6). The small size of the mapped region and the paucity of available probes frustrated attempts to define this potential replicon more thoroughly, although more recent mapping of the region centromeric to the *S* region in the mouse and between *C2* and *B144* in the human (58, 61) suggests that it should soon be possible to define the extent of the *S* region replicon. Previous analysis of this region by Hatton et al. demonstrated that in a variety of mouse cell lines, the *S* region genes replicated in the first third of S

phase with no discernible order of replication (30). Our ability to show differences in timing of replication in this regions may be due to differences in the S49.1 and WEHI-3 cells studied here compared with those cells studied by Hatton et al. Furthermore, our definitions of S1 (2.1 to 2.2C) and S2 (2.3 to 2.5C) are narrower than in this previous study of the *S* region (30), which may have facilitated detection of differences in replication early in S phase.

Insufficient data were available to define unambiguously a temporal gradient in the *D-Qa* region. The 500 kb of contiguous DNA in the *D-Qa* region offer a large region to study, but gene duplications complicate hybridization with probes for the *D* and *Qa* regions. If the discontinuity between the RHVS1s of probes 24 and 25 is interpreted as being due to deviation of the data, the entire chromosomal region between *B144* and *Q7* may constitute a single large replicon (Fig. 6, long dashes). Alternatively, a unidirectional or highly asymmetric replicon may originate at or near the transcribed *D* gene and another may originate at or near the transcribed *L* gene and extend through the *Qa* region (Fig. 6, short dashes). However, in this region the distance between probe-hybridizing sequences leaves open the possibility of additional origins.

The *T23-T16* segment of the S49.1 *TL* region also apparently indicates a temporal gradient in the range of Δ10 RHVS1/100 kb, with correspondence between replication and transcription directions (Fig. 7). Cloning and linking the region between the *T23-T16* and *T11-T1* segments and on both the centromeric side of *T23* and the telomeric side of *T1* are needed to confirm the direction and extent of *TL* replicons. The S49.1 *TL* region yielded higher RHVS1s than did the WEHI-3 *TL* region. This relative difference in replication timing could result from differences in the location of active replication origins within the *TL* regions of the two cell lines. If *TL* genes are closer to replication origins in S49.1 cells than in WEHI-3 cells, S49.1 HL DNA should have a higher RHVS1. Alternatively, the *TL* region DNA of both cell types might replicate from the same origins, but initiation of replication later in S phase in WEHI-3 cells than S49.1 cells would generate a lower RHVS1. The method used in this study cannot distinguish between these alternative explanations.

Specific sequences which initiate replication, such as *oriC* and *ARS1*, are well characterized in *Escherichia coli* and yeasts, respectively, but have proven elusive in higher eukaryotes. The best-defined mammalian origin of replication is the ori-beta initiation locus, a bidirectional origin defined within a 0.45-kb segment 17 kb downstream of the 3′ end of the DHFR gene in Chinese hamster ovary cells (8, 12). This origin shares common structural and protein binding features with the *ARS1* yeast origin of replication (9), suggesting that a specific set of sequences may initiate mammalian DNA replication. The origins of replication in the *H-2* complex cannot be mapped precisely by the temporal comparison used in this study. However, establishment of the broad definition of replicon size and replication direction is a necessary first step in the search for specific initiation sites in this large chromosomal region. Our data suggest that origins might be located near *K*, *HAM2*, *Slp*, *TNF*, and *T16*.

The definition of adjoining replicons should also facilitate analysis of how the termination of replication is controlled. Sequences which impede replication forks have been demonstrated in *E. coli* chromosomes and *E. coli* plasmids (38). It is not clear whether such terminators also exist in mammalian replicons. Mapping of replication in the DHFR region showed a coincidence between replicon junctions and association with the nuclear matrix (28). The junction between the *K* and asymmetric *I* region replicons would be a good site to use for determining the factors that regulate the termination of mammalian DNA synthesis.

The earliest relative replication sites in the *H-2* complex coincide with transcribed genes. Furthermore, the transcriptionally active *TL* region of S49.1 cells replicates earlier than does the inactive *TL* region of WEHI-3 cells. Relationships between transcription and replication have been observed in prokaryotes, mammalian viruses, and eukaryotes. For example, RNA polymerase activity precedes the initiation of replication at the *E. coli* chromosomal origin *oriC* (3). Transcriptional enhancers and binding sites for transcription factors colocalize with replication origins in a variety of viruses, including simian virus 40, bovine papillomavirus, and Epstein-Barr virus (16). Transcriptional activation of mammalian genes often changes the replication timing of the activated genes and surrounding DNA. For example, the β-globin gene cluster is transcribed and replicates early in the S phase of the human erythroid line K562 but is not transcribed and replicates late in the HeLa cell line (17). Similarly, the temporal order of replication in the IgH complex was measurable in non-B cells and allowed definition of part of a replicon, but in cells transcribing this region, the replication was too early and too rapid to measure (7). Thus, the early replication of transcribed gene regions in the *H-2* complex and the difference in the *TL* replication timing between S49.1 and WEHI-3 cells are consistent with the growing evidence of a relationship between transcription and replication. The WEHI-3 and S49.1 cell lines offer further opportunities to examine this relationship. Class II genes are not transcribed in mouse T cells, including the S49.1 cell line. In the monocyte/macrophages and their cell lines, class II transcription is induced by cytokines, including gamma interferon (52). It would be of interest to examine the effect of these cytokines on replication in the *I* region replicon of WEHI-3 myelomonocyte cells. The correlation between class I gene expression (*K*, *D*, and *L*) and early replication can be examined in several S49.1 sublines with differential class I expression (34). Further characterization of the genes recently identified in the *Pb-Ob* segment (13) should resolve whether the difference in the RHVS1 of S49.1 and WEHI HL DNA hybridizing with probe 10 was due to transcriptional differences in genes *Mb1* and *Mb2* (*m* and *l*, respectively, in Fig. 5).

The earliest relative replication in the *H-2* complex resulted in RHVS1s of 60 to 68. Several gene regions gave these results, including DNA in the vicinity of *HAM1*, *Ob*, *Slp*, *B144*, *TNF*, *D*, and *T16*. Within the limits of resolution of our temporal measurements, replicons in these regions seem to have initiated DNA synthesis during similar portions of the S phase. Clusters of synchronized replicons have been observed in a wide range of eukaryotes (reviewed in reference 27). The *H-2* complex contains >2,000 kb of cloned DNA, with a potential for over 1,000 kb more when gaps between the regions are filled. The *H-2* complex is therefore significantly larger than other mammalian chromosomal segments in which replication has been examined, including the 150-kb β-globin gene region (17), 300-kb IgH region (7), 240- and 650-kb amplified DHFR domains (8, 18, 44), and 500-kb cystic fibrosis gene region (59). Analysis of replication in the *H-2* complex affords an unique opportunity to study the coordinated regulation of a replicon cluster.

The lowest RHVS1 in the *H-2* complex, and hence the latest replication, was measured in the *Hmt* region gene *M1*.

Because the *Hmt* region has not been mapped, we could not determine whether *M1* is far from a replication origin which initiates at the same time as do the other *H-2* origins or whether it is part of a replicon which initiates later in S phase than do those in *K* to *TL*. The *Hmt* region is located in G-band-like interchromomere region B of chromosome 17, whereas most of the *H-2* complex lies in R-band-like chromomere band C (39). G-band chromatin generally replicates later than R-band chromatin (31), so further analysis of *Hmt* region replication may provide insights into the coordination of replicon clusters and the effect of general chromatin properties on DNA replication.

Several previous studies have suggested a relationship between replication and recombination in eukaryotic viruses and in eukaryotic chromosomes. For example, in bacteriophage T4, two recombination hot spots coincide with origins of replication (37). Several models of mammalian chromosomal recombination have proposed that sister chromatid exchanges occur during disruption of DNA replication and that crossover points occur at junctions between adjacent replicons or replicon clusters (14, 42). Meiotic recombination in the MHC is not random. Rather, long stretches of the MHC do not contain any documented recombination sites, while many of the independent crossover events have been mapped to a few short DNA segments (64, 65). One such hotspot of homologous recombination, observed in heterozygotes involving the *b*, *d*, *f*, *k*, and *s* haplotypes, occurs within a 2.9-kb segment in the second intron of the *Eb* gene (74). We sought to determine whether this recombination hot spot in meiotic cells corresponds to a replication origin or termination point in the S phase of mitotic somatic cells. Our replicon mapping studies do not show anything unusual about the timing of *Eb* replication in the *d* haplotype WEHI-3 and S49.1 cells. In both of these somatic cell lines, the *Eb* gene is located in the middle of a particularly large apparent replicon in a position clearly distant from the apparent origin and terminus of replication. Within the limits of resolution of our methods, there is no evidence of a pause in the replication of this gene. We cannot resolve whether this portion of the MHC is susceptible to infrequent disruptions in DNA synthesis. Furthermore, we do not know whether this replicon is identical in the germ cells in which meiotic recombination occurs. Our data, as well as those from several previous studies, show that the portion of S phase in which a particular chromosomal region is replicated can vary among different cell types. Therefore, we cannot exclude the possibility that the *Eb* recombinational hot spot coincides with a distinct feature of replication in germ cells.

The class I genes *K*, *D*, and *L* and the class II genes *Aa*, *Ab*, and *Eb* are extremely polymorphic. This allelic polymorphism affects the ability of these proteins to bind and present antigenic peptides to T cells. The segments of the *K*, *D*, and *I* regions containing these genes have relatively high restriction enzyme site polymorphism (62). In contrast, the *S*, *Qa*, and *TL* regions are much less polymorphic in both genes and intergenic regions among different haplotypes. Comparison of RHVS1s indicates that segments of polymorphic and conserved *H-2* regions are replicated during the same portions of S phase. We did, however, find several correlations between replicons and regions containing related genes. For example, the class II genes of the *I* region appear to replicate as part of a single unit. The *S*, *D*, and *Qa* regions may also constitute separate replicons. If so, the gene duplications which expanded these regions did not disrupt the replicons.

The replicon mapping results presented here represent a first order of resolution and should provide a basis for finer mapping techniques (18, 28, 59, 71). The size and extensive characterization of the *H-2* complex offer unique opportunities to study the control of mammalian DNA replication.

ACKNOWLEDGMENTS

We gratefully thank the following individuals for their generous contributions of MHC region cosmids and DNA probes: Kurt Brorson, Elaine Gese, and Lee Hood (California Institute of Technology); Michael Steinmetz (F. Hoffmann-La Roche & Co.); Julie Vogel, Suzanne Watts, and Robert Goodenow (University of California, Berkeley); Karen Artzt (University of Texas at Austin); Ronald Ogato (Scripps Clinic and Research Foundation); Bruce Dowton and Harvey Colten (Washington University School of Medicine); Fung-Win Shen (Showa University Research Institute for Biomedicine in Florida); Dinah Singer (National Institutes of Health); and Barbara Hamkalo (University of California, Irvine). Fluorescence-activated cell sorting analyses were skillfully performed by Catherine Carswell-Crumpton and Larry Seamer.

This research was supported by NIH grants AG05568 and GM 14931.

REFERENCES

1. **Abe, K., J.-F. Wei, F.-S. Wei, Y.-C. Hsu, H. Uehara, K. Artzt, and D. Bennett.** 1988. Searching for coding sequences in the mammalian genome: the H-2K region of the mouse MHC is replete with genes expressed in embryos. EMBO J. **7**:3441–3449.
2. **Anachkova, B., and J. L. Hamlin.** 1989. Replication in the amplified dihydrofolate reductase domain in CHO cells may initiate at two distinct sites, one of which is a repetitive sequence element. Mol. Cell. Biol. **9**:532–540.

2a. **Artzt, K.** Personal communication.

3. **Baker, T. A., and A. Kornberg.** 1988. Transcriptional activation of initiation of replication from the E. coli chromosomal origin: an RNA-DNA hybrid near oriC. Cell **55**:113–123.
4. **Blumenthal, A. B., H. J. Kriegstein, and D. S. Hogness.** 1974. The units of DNA replication in *Drosophila melanogaster* chromosomes. Cold Spring Harbor Symp. Quant. Biol. **38**:205–223.
5. **Brorson, K. A., S. W. Hunt III, T. Hunkapiller, Y. H. Sun, H. Cheroutre, D. A. Nickerson, and L. Hood.** 1989. Comparison of exon 5 sequences from 35 class I genes of the BALB/c mouse. J. Exp. Med. **170**:1837–1858.
6. **Brorson, K. A., S. Richards, S. W. Hunt III, H. Cheroutre, K. Fischer Lindahl, and L. Hood.** 1989. Analysis of a new class I gene mapping to the Hmt region of the mouse. Immunogenetics **30**:273–283.
7. **Brown, E. H., M. A. Iqbal, S. Stuart, K. S. Hatton, J. Valinsky, and C. L. Schildkraut.** 1987. Rate of replication of the murine immunoglobulin heavy-chain locus: evidence that the region is part of a single replicon. Mol. Cell. Biol. **7**:450–457.
8. **Burhans, W. C., L. T. Vassilev, M. S. Caddle, N. H. Heintz, and M. L. DePamphilis.** 1990. Identification of an origin of bidirectional DNA replication in mammalian chromosomes. Cell **62**: 955–965.
9. **Caddle, M. S., L. Dailey, and N. H. Heintz.** 1990. RIP60, a mammalian origin-binding protein, enhances DNA bending near the dihydrofolate reductase origin of replication. Mol. Cell. Biol. **10**:6236–6234.
10. **Calza, R. E., L. A. Eckhardt, T. DelGiudice, and C. L. Schildkraut.** 1984. Changes in gene position are accompanied by a change in time of replication. Cell **36**:689–696.
11. **Chaplin, D. D., D. E. Woods, A. S. Whitehead, G. Goldberger, H. R. Colten, and J. G. Seidman.** 1983. Molecular map of the murine S region. Proc. Natl. Acad. Sci. USA **80**:6947–6951.
12. **Chi, M., T.-H. Lev, and J. L. Hamlin.** 1990. Multiple origins of replication in the dihydrofolate reductase amplicons of a methotrexate-resistant Chinese hamster cell line. Mol. Cell. Biol. **10**:1338–1346.
13. **Cho, S., M. Attaya, M. G. Brown, and J. L. Monaco.** 1991. A cluster of transcribed sequences between the Pb and Ob genes of the murine major histocompatibility complex. Proc. Natl.

Acad. Sci. USA **88**:5197–5201.
14. **Cleaver, J. E.** 1981. Correlations between sister chromatid exchange frequencies and replicon sizes. Exp. Cell Res. **136**: 27–30.
15. **Davis, M. M., D. I. Cohen, E. A. Nielsen, M. Steinmetz, W. E. Paul, and L. Hood.** 1984. Cell-type-specific cDNA probes and the murine I region: the localization and orientation of A_α^d. Proc. Natl. Acad. Sci. USA **81**:2194–2198.
16. **DePamphilis, M. L.** 1988. Transcriptional elements as components of eukaryotic origins of DNA replication. Cell **52**:635–638.
17. **Dhar, V., D. Mager, A. Iqbal, and C. L. Schildkraut.** 1988. The coordinate replication of the human β-globin gene domain reflects its transcriptional activity and nuclease hypersensitivity. Mol. Cell. Biol. **8**:4958–4965.
18. **Dijkwel, P. A., J. P. Vaughn, and J. L. Hamlin.** 1991. Mapping of replication initiation sites in mammalian genomes by two-dimensional gel analysis: stabilization and enrichment of replication intermediates by isolation on the nuclear matrix. Mol. Cell. Biol. **11**:3850–3859.
19. **Edenberg, H. J., and J. A. Huberman.** 1975. Eukaryotic chromosome replication. Annu. Rev. Genet. **9**:245–284.
20. **Estess, P., A. B. Begovich, M. Koo, P. P. Jones, and H. O. McDevitt.** 1986. Sequence analysis and structure-function correlations of murine q, k, u, s, and f haplotype IA b cDNA clones. Proc. Natl. Acad. Sci. USA **83**:3594–3598.
21. **Falus, A., E. K. Wakeland, T. J. McConnell, J. Gitlin, A. S. Whitehead, and H. R. Colten.** 1987. DNA polymorphism of MHC III genes in inbred and wild mouse strains. Immunogenetics **25**:290–298.
22. **Feinberg, A. P., and B. Vogelstein.** 1983. A technique for radiolabelling DNA restriction endonuclease fragments to high specificity. Anal. Biochem. **132**:6–13.
23. **Fisher, D. A., S. W. Hunt III, and L. Hood.** 1985. Structure of a gene encoding a murine thymus leukemia antigen, and organization of *Tla* genes in the BALB/c mouse. J. Exp. Med. **162**:528–545.
24. **Furst, A., E. H. Brown, J. D. Braunstein, and C. L. Schildkraut.** 1981. α-Globin sequences are located in a region of early replicating DNA in murine erythroleukemia cells. Proc. Natl. Acad. Sci. USA **78**:1023–1027.
25. **Goldman, M. A., G. P. Holmquist, M. C. Gray, L. A. Caston, and A. Nag.** 1984. Replication timing of genes and middle repetitive sequences. Science **224**:686–692.
26. **Hagen, K. T. G., D. M. Gilbert, H. F. Willard, and S. N. Cohen.** 1990. Replication timing of DNA sequences associated with human centromeres and telomeres. Mol. Cell. Biol. **10**:6348–6355.
27. **Hand, R.** 1978. Eukcaryotic DNA: organization of the genome for replication. Cell **15**:317–325.
28. **Handeli, S., A. Klar, M. Meuth, and H. Cedar.** 1989. Mapping replication units in animal cells. Cell **57**:909–920.
29. **Hanson, I. M., and J. Trowsdale.** 1991. Colinearity of novel genes in the class II regions of the *MHC* in mouse and human. Immunogenetics **34**:5–11.
30. **Hatton, K. S., V. Dhar, E. H. Brown, M. A. Iqbal, S. Stuart, V. T. Didamo, and C. L. Schildkraut.** 1988. Replication program of active and inactive multigene families in mammalian cells. Mol. Cell. Biol. **8**:2149–2158.
31. **Holmquist, G. P.** 1989. Evolution of chromosomal bands: molecular evolution of noncoding DNA. J. Mol. Evol. **28**:469–486.
32. **Horibata, K., and A. W. Harris.** 1970. Mouse myelomas and lymphomas in culture. Exp. Cell Res. **60**:61–77.
33. **Huberman, J. A., and A. D. Riggs.** 1968. On the mechanism of DNA replication in mammalian chromosomes. J. Mol. Biol. **32**:327–341.
34. **Keeney, J. B., M. Hedayat, N. M. Myers, J. M. Connolly, and T. H. Hansen.** 1989. Locus-specific regulation of K^d, D^d and L^d class I genes in the BALB/c S49 lymphoma sublines. J. Immunol. **143**:2364–2373.
35. **Klein, J., C. Benoist, C. S. David, P. Demant, K. Fischer Lindahl, L. Flaherty, R. A. Flavell, U. Hammerling, L. E. Hood, S. W. Hunt III, P. P. Jones, P. Kourilsky, H. O. McDevitt, D. Meruelo, D. B. Murphy, S. G. Nathenson, D. H. Sachs, M. Steinmetz, S. Tonegawa, E. K. Wakeland, and E. H. Weiss.** 1990. Revised nomenclature of mouse H-2 genes. Immunogenetics **32**:147–149.
36. **Klein, J., F. Figueroa, and C. S. David.** 1983. *H-2* haplotypes, genes, and antigens: second listing. Immunogenetics **17**:553–596.
37. **Kreuzer, K. N., and B. M. Alberts.** 1985. A defective phage system reveals bacteriophage T4 replication origins that coincide with recombination hot spots. Proc. Natl. Acad. Sci. USA **82**:3345–3349.
38. **Kuempel, P. L., A. J. Pelletier, and T. M. Hill.** 1989. Tus and the terminators: the arrest of replication in prokaryotes. Cell **59**: 581–583.
39. **Lader, E., B. T. Clark, A. C. Jhanwar, R. S. K. Chaganti, and D. Bennett.** 1985. Definitive chromosomal location of the H-2 complex by in situ hybridization to pachytene chromosomes. Immunogenetics **22**:49–54.
40. **Lai, E., R. K. Wilson, and L. E. Hood.** 1989. Physical maps of the mouse and human immunoglobulin-like loci. Adv. Immunol. **46**:1–59.
41. **Leffak, M., and C. D. Jams.** 1989. Opposite replication polarity of the germ line c-*myc* gene in HeLa cells compared with that of two Burkitt lymphoma cell lines. Mol. Cell. Biol. **9**:586–593.
42. **Lugo, M. H., H. S. Rauchfoss, H. R. Zakour, J. W. Allen, and J. C. Hozier.** 1989. Evidence for chromosomal replicons as units of sister chromatid exchanges. Chromosoma **98**:69–76.
43. **Linskens, M. H. K., and J. A. Huberman.** 1990. The two faces of higher eukaryotic DNA replication origins. Cell **62**:845–847.
44. **Ma, C., T.-H. Leu, and J. L. Hamlin.** 1990. Multiple origins of replication in the dihydrofolate reductase amplicons of a methotrexate-resistant Chinese hamster cell line. Mol. Cell. Biol. **10**:1338–1346.
45. **Mathis, D. J., C. O. Benoist, V. E. Williams, M. R. Kanter, and H. O. McDevitt.** 1983. The murine E alpha immune response gene. Cell **32**:745–754.
46. **Mengle-Daw, L., and H. O. McDevitt.** 1983. Isolation and characterization of a cDNA clone for the I-E beta polypeptide chain. Proc. Natl. Acad. Sci. USA **80**:7621–7625.
46a. **Monaco, J.** Personal communication.
47. **Monaco, J. J., S. Cho, and M. Attaya.** 1990. Transport protein genes in the murine MHC: possible implications for antigen processing. Science **250**:1723–1726.
48. **Muller, U., D. Stephan, P. Phillippsen, and M. Steinmetz.** 1987. Orientation and molecular map position of the complement genes in the mouse MHC. EMBO J. **6**:369–373.
49. **Ogata, R. T., and D. S. Sepich.** 1984. Genes for murine fourth complement component (C4) and sex-limited protein (Slp) identified by hybridization to C4- and Slp-specific cDNA. 1984. Proc. Natl. Acad. Sci. USA **81**:4908–4911.
50. **Ogata, R. T., D. C. Shreffler, D. S. Sepick, and S. P. Lilly.** 1983. cDNA clone spanning the α-γ subunit junction in the precursor of the murine fourth complement component (C4). Proc. Natl. Acad. Sci. USA **80**:5061–5065.
51. **Passmore, H. C., and J. Romano.** 1988. Genetic organization of the *Qa* and *Tla* regions: gene mapping based on the analysis of recombinant strains, p. 49–60. *In* C. S. David (ed.), Major histocompatibility genes and their role in immune functions. Plenum Publishing, New York.
52. **Paulnock-King, D., K. C. Sizer, Y. R. Freund, P. P. Jones, and J. R. Parnes.** 1985. Coordinate induction of Ia alpha, beta, and Ii mRNA in a macrophage cell line. J. Immunol. **135**:632–636.
53. **Pennica, D., J. S. Hayflick, T. S. Bringman, M. A. Palladino, and D. V. Goeddel.** 1985. Cloning and expression in Escherichia coli of the cDNA for murine tumor necrosis factor. Proc. Natl. Acad. Sci. USA **82**:6060–6064.
54. **Radic, M. Z., K. Lundgren, and B. A. Hamkalo.** 1987. Curvature of mouse satellite DNA and condensation of heterochromatin. Cell **50**:1101–1108.
55. **Richards, S., M. Bucan, K. Brorson, M. C. Kiefer, S. W. Hunt III, H. Lehrach, and K. Fischer Lindahl.** 1989. Genetic and molecular mapping of the *Hmt* region of mouse. EMBO J. **8**:3749–3757.
56. **Rogers, J. H., M. F. Lyon, and K. R. Willison.** 1985. The

arrangement of *H-2* class I genes in mouse t haplotypes. J. Immunogenet. **12**:151–165.
57. **Rogers, J. H., and K. R. Williams.** 1983. A major rearrangement in the H-2 complex of mouse *t* haplotypes. Nature (London) **304**:549–552.
58. **Sargent, C. A., I. Dunham, and R. D. Campbell.** 1989. Identification of multiple HTF-island associated genes in the human major histocompatibility complex class III region. EMBO J. **8**:2305–2312.
59. **Selig, S., K. Okumura, D. C. Ward, and H. Cedar.** 1992. Delineation of DNA replication time zones by fluorescence in situ hybridization. EMBO J. **11**:1217–1225.
60. **Singer, D. S., J. Hare, H. Golding, L. Flaherty, and S. Rudikoff.** 1988. Characterization of a new subfamily of class I genes in the H-2 complex of the mouse. Immunogenetics **28**:13–21.
60a. **Spack, E. G., B. Kusler, and P. P. Jones.** Unpublished data.
61. **Spies, T., M. Bresnahan, and J. L. Strominger.** 1989. Human major histocompatibility complex contains a minimum of 19 genes between the complement cluster and HLA-B. Proc. Natl. Acad. Sci. USA **86**:8955–8958.
62. **Steinmetz, M., M. Malissen, L. Hood, A. Orn, R. A. Maki, G. R. Dastoornikoo, D. Stephan, E. Gibb, and R. Romaniuk.** 1984. Tracts of high or low sequence divergence in the mouse major histocompatibility complex. EMBO J. **3**:2995–3003.
63. **Steinmetz, M., K. Minard, S. Horvath, J. McNicholas, J. Srelinger, C. Wake, E. Long, B. Mach, and L. Hood.** 1982. A molecular map of the immune response region from the major histocompatibility complex of the mouse. Nature (London) **300**:35–42.
64. **Steinmetz, M., D. Stephan, and K. Fischer Lindahl.** 1986. Gene organization and recombinational hotspots in the murine major histocompatibility complex. Cell **44**:895–904.
65. **Steinmetz, M., Y. Uematsu, and K. Fischer-Lindahl.** 1987. Hotspots of homologous recombination in mammalian genomes. Trends Genet. **4**:59–62.
66. **Steinmetz, M., A. Winoto, K. Minard, and L. Hood.** 1982. Clusters of genes encoding mouse transplantation antigens. Cell **28**:489–498.
67. **Stephan, D., H. Sun, K. Fischer Lindahl, E. Meyer, G. Hammerling, L. Hood, and M. Steinmetz.** 1986. Organization and evolution of D region class I genes in the mouse major histocompatibility complex. J. Exp. Med. **163**:1227–1244.
68. **Tsuge, I., F.-W. Shen, M. Steinmetz, and E. A. Boyse.** 1987. A gene in the H-2A:H-2D interval of the major histocompatibility complex which is transcribed in B cells and macrophages. Immunogenetics **26**:378–380.
69. **Uehara, H., K. Abe, C.-H. Park, H.-S. Shin, D. Bennett, and K. Artzt.** 1987. The molecular organization of the H-2K region of two t-haplotypes: implications for the evolution of genetic diversity. EMBO J. **6**:83–90.
70. **Umek, R. M., M. H. K. Linskens, D. Kowalski, and J. A. Huberman.** 1989. New beginnings in studies of eukaryotic DNA replication origins. Biochim. Biophys. Acta **1007**:1–14.
71. **Vassilev, L., and E. M. Johnson.** 1989. Mapping initiation sites of DNA replication *in vivo* using polymerase chain reaction amplification of nascent strand segments. Nucleic Acids Res. **17**:7693–7705.
72. **Vaughn, J. P., P. A. Dijkwel, and J. L. Hamlin.** 1990. Replication initiates in a broad zone in the amplified CHO dihydrofolate reductase domain. Cell **61**:1075–1087.
73. **Winoto, A., M. Steinmetz, and L. Hood.** 1983. Genetic mapping in the major histocompatibility complex by restriction enzyme site polymorphisms: most mouse class I genes map to the Tla complex. Proc. Natl. Acad. Sci. USA **80**:3425–3429.
74. **Zimmerer, E. J., and H. C. Passmore.** 1991. Structural and genetic properties of the Eb recombinational hotspot in the mouse. Immunogenetics **33**:132–140.